Electrical Engineering Project 2102499

Classification on Knee Medical Condition from Vibration Signals

Tanut Aranchayanont 5531029221
SRA: Advance Control and Optimization
Jitkomut Songsiri

Department of Electrical Engineering
Faculty of Engineering
Chulalongkorn University
Academic Year 2015

Contents

1 Introduction

Nowadays, knee diseases diagnoses are only carried out by orthopaedic physician. If further information is needed for diagnostic purpose, invasive and complicated methods are introduced, for example arthoscopic, MRI, X-ray. Consequently, patients will have an examination only when they have a symptom. However, knee diseases are prevalent as much as 22.7% of the adult population [1] so that an early detection is needed for an early treatment before developing into a stage that has symptoms.

According to a common practice on knee condition diagnostic, sound and vibration are main factors physicians concern. Such practice and earlier literature motivate a classification method based on *Vibroartrographic signals* (VAG signals), a knee vibration signal. Vibration arthrometry is a study of sounds or vibrations naturally produced by a joint while in motion. One of the instrument using to measure a VAG signal from a knee is a piezoelectric accelerometer. The accelerometer is a contact sensor so that it can overcome the background noise problem [2]. As an example to illustrate the nature of VAG signal, data from *resurface* and *non-resurface* class are considered.

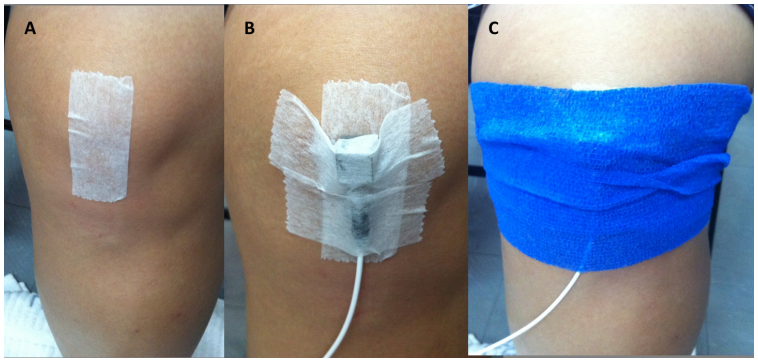

Figure 1: An accelerometer attachment: First, the mid-patella position is indicated by physician as in A. Then accelerometer is attached and fixed by tape horizontally and vertically as in B. Finally a bandage is fasten to make the attachment firm as in C.

Both resurface and non-resurface classes of VAG signals belong to subjects whom received knee joint replacement, shown as a metallic object in Figure 2a. The difference is that the resurface class subject further received a *patella* replacement, shown as a white circular shape object in Figure 2a. A knee structure and a position of patella are shown in Figure 2b. A knee joint replacement is a main treatment of knee diseases and we hypothesize that a patella replacement results in smoother VAG signals.

In the experiment, an accelerometer is attached to the mid-patella position of the knee, as shown in Figure 1. Subjects were asked to sit on the flat surface with legs suspending in the air. Before the measurement, the subjects were rested for 5 minutes. This is because a prior movement in knee causes VAG signals to become *smoother* [3]. However, after 5 minutes of rest, the knee will return to its initial condition [2].

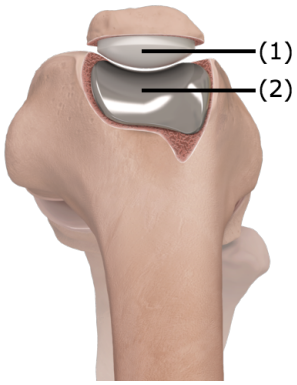

(a) A drawing of resurface class knee structure shows: (1) a patella replacement with a white circular shape object, (2) a knee joint replacement with a metallic object. A patella position is labeled by 10 in Figure 2b

https://www.arthrex.com/newsroom/blog/2013/10/28/patellofemoral-joint-arthroplasty-pfj

.

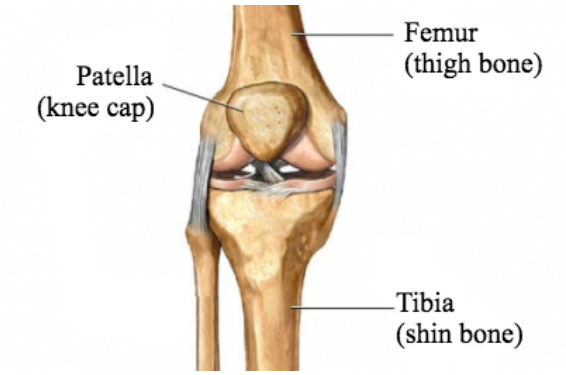

(b) The structure of human knee. Femur, Tibia and Patella are indicated with number $1, 5$ and 10 respectively. Photo from Web Anatomy, University of Minnesota.

http://msjensen.cehd.umn.edu/webanatomy/skeletal/bone_knee_4_answers.html

Figure 2: Overview of a knee structure and parts that receive operations for non-resurface and resurface class.

The subjects were assisted to extend and flex their legs. An assistance to the subject movement is required to control the frequency of each cycle. Suppose that the line parallel to subject lap is $0°$, one flexion-extension cycle contains movement from $0°$ to $90°$ and back to $0°$. An iteration of measurement approximately contains $9 - 15$ cycles. Note that VAG signals are sinusoidal due to the measurement process. Let x be a displacement relative to 0 degree line and let ω to be a constant. Ignoring the micro-vibration, the simplest equation describing VAG signals is:

$$x(t) = A\sin(\omega t + \phi), \quad \ddot{x}(t) = -A\omega^2 \sin(\omega t + \phi). \tag{1}$$

From (1), it is obvious that ω has an effect on the amplitude of the VAG signal. So that speed of flexion-extension cycle should be controlled. Furthermore, the literature [4, 5] considered that VAG signals are emitted from different structures at different knee angle and different times. In the measurement process, we can control ω to be a constant to keep the VAG signal as periodic as possible. This is important for time-frequency analysis of processed VAG signal in section 3.2

Plots of VAG signals of non-resurface and resurface classes are shown in Figure 3a and 3b. VAG signals contain three main components as follows: (i) Acceleration from motion which will be called motion trend through out this paper. The simplest model of such motion is described by (1). (ii) Micro vibration from knee joint. Such vibration can be measured in form of an acceleration. Measured VAG signals consist of the sound of Femur, Patella,

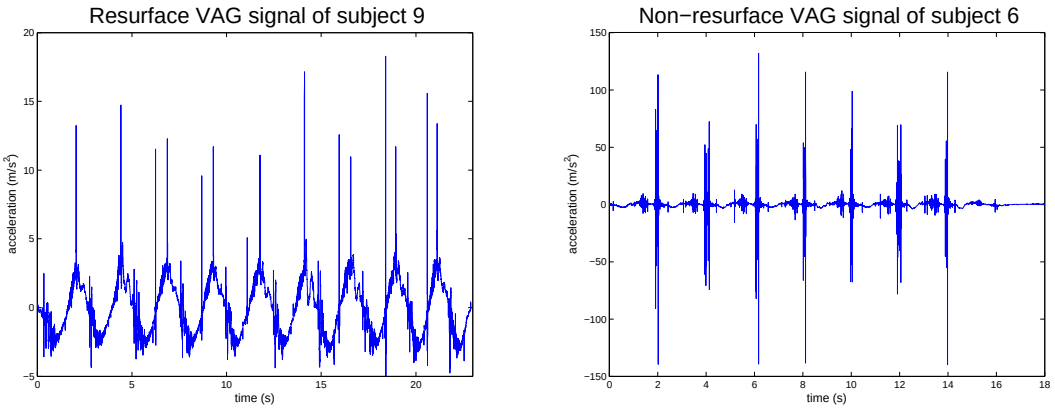

(a) Resurface VAG signal (b) Non-resurface VAG signal

Figure 3: Example of VAG signals. The spikes in VAG signals occur due to the implosion of bubble in synovial fluid.

and Tibia rubbing to each other. This vibration originate from the inner structure of knee. The location of Femur, Tibia and Patella are indicated by number $1, 5$ and 10 in Figure 2b. (iii) Spikes which are the high magnitude components occuring periodically at the either beginning or end of the flexion-extension cycle.

In the literature, there are attempts to classify VAG signals to represent distinctions between a *normal* and *abnormal* knee. Examples of abnormal classes are: rheumatoid arthritis, osteoarthritis, chondromalacia patella and meniscus tear [4, 5]. An assumption suggested by the studies is that abnormal VAG signals are *noisier* than the normal signals. The term noisy can be viewed as high amplitude of acceleration [6]. In Kernohan et al. work [6], the range of an acceleration reduces from more than 15 to $1.7m/s^2$ after the subject receive a surgery. In the work of Chu et al. [7], the frequency of abnormal class spread through the audible range ($20 - 20000$ Hz). Normal knees were found to have a very low value of acoustic power while those with rheumatoid arthritis have higher values and those with degenerative arthritis were highest of all. The amplitude of the signal seemed to correlate with the severity of cartilage damage observed.

The example plot of resurface and non-resurface VAG signals are shown in Figure 3. A spike in VAG signal is suspectd to be a result of implosion of bubble in synovial fluid causing a slip-stick vibration. The resurface VAG signal in Figure 3a appears to be relatively smooth. In contrast, the non-resurface VAG signal in Figure 3b shows high acceleration magnitude. Also, it is reported that the physician can hear a *crepitus* sound which indicates a degraded knee.

Both literature and the data sets suggest that the frequency components higher than 1000 Hz are normally below -100 dBW, which we consider to be too low for consideration. Therefore we would propose an analysis restricted to frequency below 1000 Hz. Likewise, our hypothesis on the key characteristics of VAG signals will only concern components in range of $0 - 1000$ Hz.

From an available data set of resurface and non-resurface, the project aims to analyse spectral properties of VAG signals together with discussing their difference and similarity. Due to motion trend and noise in raw VAG signals, signal processing technique must be first applied. The processing technique used to clean the raw signal are described in section 2. From spectral overview of resurface/non-resurface data set, noise are spread over interested frequency band. Moreover, VAG signal is non-stationary; therefore, it should be processed with non-stationary signal processing technique. In this case, we choose EEMD (Ensemble Empirical Mode Decomposition). EEMD is used to decompose signal into a set of modes. After that, the DFA (Detrended Fluctuation analysis) technique is used to analyse correlation properties of each modes. The objective of DFA is to differentiate intrinsic signal and noise. Finally the processed signals are analysed with STFT (Short Time Fourier Transform) to observe time-frequency characteristics.

2 Processing Pipeline

Similar to other physiological signal, VAG signals collected are inevitably contaiminated by noise, for example, from muscle contraction [3]. Besides, there also components that is irrelevant to the characteristics of VAG signal such as motion trend. Thus, a processing pipeline is introduced to filter out the motion trend and noise especially the one which spread over the frequency band. The whole pipeline is illustrated in Figure 4. First, motion trend is eliminated with basic filtering technique. Since VAG signal is non-stationary, it should be fed to processed with non-stationary signal processing technique in the next block. Among available techniques, EEMD [8] is widely used with physiological signals such as ECG signal (Electrocadiograph signal) [9]. So EEMD is chosen to be a processing block after high pass filter block. After obtaining a set of signal from EEMD, the signal which shows randomness should be discarded before being composed back. Therefore, DFA [10] is introduced to determine such randomness with parameter α. In other word, DFA determine how *correlated* a signal is. We choose the criterion $\alpha \leq 0.5$ to discard uncorrelated signals. Finally, the set of signals that pass the criterion will be composed back to be processed signal $x_{\text{processed}}$. There is also a spike extraction block that preserve spikes before the signal undergoes the EEMD block. Additionally spike extraction make each IMFs easier to observe. In order to analyse processed VAG signal, STFT (Short Time Fourier Transform) is used. With STFT, information are obtained in both time and frequency. So that it is possible to observe frequency and change of frequency in each flexion-extension cycle.

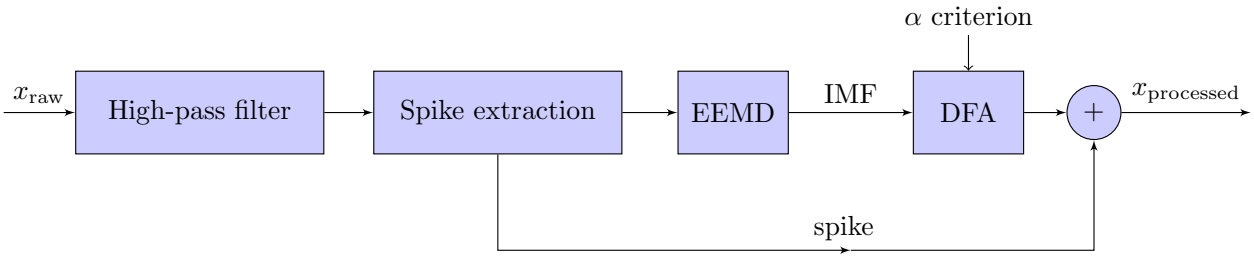

Figure 4: VAG signal processing pipeline.

2.1 High-pass filter

High-pass filter aims to eliminate the motion trend in VAG signals, which is generated from flexion-extension cycle. Since flexion-extension cycle is controlled to have a period about $1s$, the motion trend will have low frequency and can be filtered out easily by high-pass filter. IIR Butterworth filter of order 2 is used to filter out the motion trend. Filter specification is as follow: $A_{\text{stop}} = -80dB, A_{\text{pass}} = 1dB, f_{\text{top}} = 1, f_{\text{pass}} = 2$. From the given data set, there exists both sinusoidal motion trend as in Figure 5a and motion trend that slightly differ from sinusoidal as in Figure 5b. Despite the variation in motion trend, high pass filter applies well for either cases.

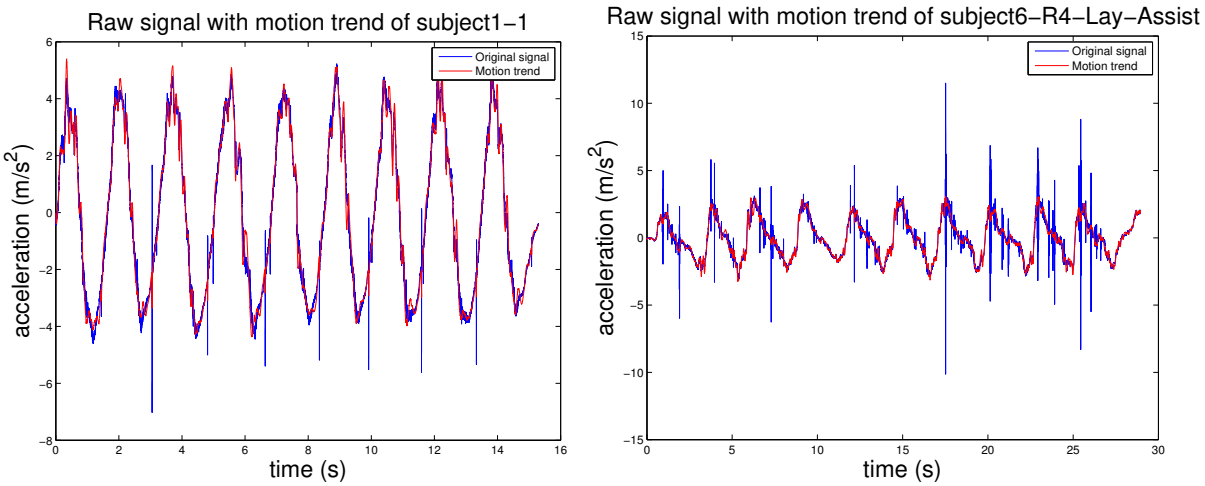

(a) Sinusoidal motion trend (b) Approximately sinusoidal motion trend

Figure 5: Example of original signal is in blue and the motion trend is in red.

2.2 Ensemble Empirical Mode Decomposition (EEMD)

This subsection will explain EEMD and EMD, non-stationary signal processing technique. EEMD is an improvement of EMD technique and mainly contains EMD subroutine. Therefore; EMD will be explained first then followed by EEMD. EMD technique is based on an assumption that a signal at any given time may contain many oscillatory modes of different frequencies. The method decomposes the signal into several components called *intrinsic mode function* (IMF) which satisfies the following two conditions:

1. the number of extrema and the number of zero crossing must either be equal or differ at most by one;

2. at any time point, the mean value of the envelope defined using the local maxima and the envelope defined using the local minima is zero.

The decomposition can be done through a *sifting process* which can be described as follows. Let $x(t)$ be an arbitrary raw signal fed to this process.

1. Identify maxima and minima of $x(t)$.

2. Connect all the local maxima (and minima) by a cubic spline line. This forms the upper and lower envelopes and the signal $x(t)$ lies between these two envelopes.

3. Calculate the mean between the two envelopes, denoted by m_1 and define $h_1 = x(t) - m_1$ as the first protomode.

4. We expect that h_1 to satisfy the properties of the IMF but it generally does not, so we repeat the process of fitting the cubic spline where in the next iteration we treat h_1 as the new input. Hence, we repeat

$$\begin{aligned} h_{11} &= h_1 - m_{11} \\ h_{12} &= h_{11} - m_{12} \\ &\vdots \quad\quad \vdots \\ h_{1k} &= h_{1(k-1)} - m_{1k} \end{aligned}$$

   until the condition on the local envelope symmetry of the IMF function is satisfied, *i.e.*, h_{1k} becomes the IMF function and defined as c_1;

$$c_1 = h_{1k}$$

   which is the first IMF component. Several stopping criterions in the sifting process have been proposed [11] such as a small relative change in $h_k(t)$ or a small sum-squared amplitude of m_{1k}.

Once the first IMF is obtained, which should contain the shortest-period oscillation, we compute the residual

$$r_1 = x(t) - c_1$$

which still consists of longer-period oscillations. This residual is then treated as the *new data* and applied to the sifting process again and obtain the second IMF, c_2. We repeat this process to obtain the residuals:

$$\begin{aligned} r_2 &= r_1 - c_2 \\ r_3 &= r_2 - c_3 \\ &\vdots \quad\quad \vdots \\ r_n &= r_{n-1} - c_n \end{aligned}$$

and stop when the residual of the nth iteration becomes a monotonic function where no more IMF can be extracted. As a result, the original signal can be written as

$$x(t) = \sum_{k=1}^{n} c_k(t) + r_n$$

where $x(t)$ can be decomposed as n IMFs with a residual r_n. We note that in EMD method, removing a constant mean from the input signal is not required since the zero reference is calculated during the sifting process. An example of sifting process is shown in Figure 6.

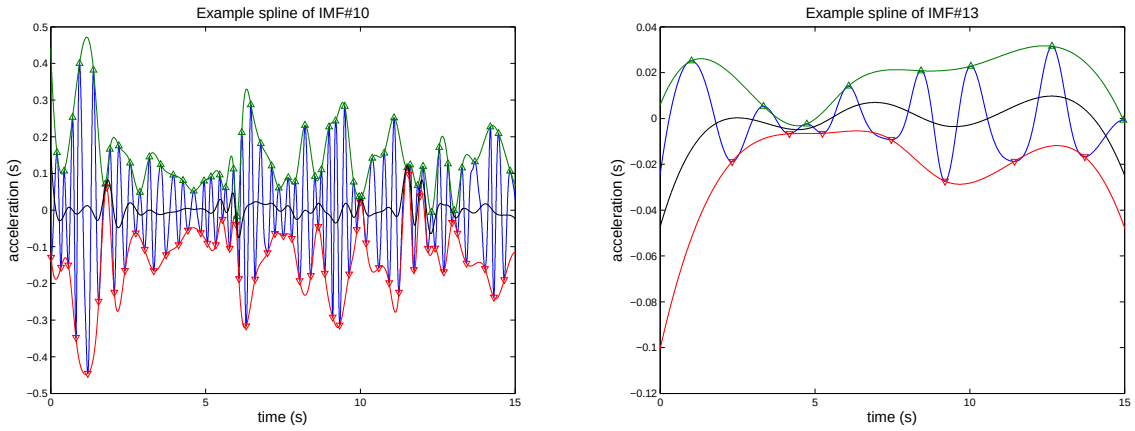

(a) Spline of IMF#10 (b) Spline of IMF#13

Figure 6: As an example, the sifting process are explained as follow. First, local maxima and minima are identified by green and red triangle. Second, the upper envelope and lower envelope are interpolated by cubic spline function depicted by green line and red line correspondingly. Mean m_{11} of upper and lower envelope is evaluated and plotted in black. Third, the signal is subtracted by the mean of the envelope to obtain h_{11}. Forth, steps are repeated until there obtains IMF. In this case, the number of zero-crossing and the number of sifting process are chosen to be the stopping criterion of the sifting process.

It is not common that EMD is implemented alone but rather carried out through the standard technique called EEMD. EEMD technique is introduced to overcome mode mixing and improve the stability of EMD technique [8]. Literally, EEMD implement EMD for N iteration. The process is explained in steps followed:

1. Mixing with white noise: Raw input signal $x(t)$ is mixed with white noise to become input signal of k^{th} iteration
$$x_k(t) = x(t) + w(t),$$
where $w(t) \sim \mathcal{N}(0, 1)$. The magnitude of white noise is normally chosen to be one standard deviation of the input signal.

2. EMD subroutine: The input signal of k^{th} iteration $x_k(t)$ is applied with EMD technique yielding a set of IMF of k^{th} iteration $\{c_{k,1}, c_{k,2}, c_{k,3}, \ldots, c_{k,n}\}$.

3. Average signal from all iteration: The IMF resulting from each iteration are averaged to obtain the single IMF result. For example IMF#1 is evaluated by $c_1 = \sum_{k=1}^{N} c_{k,1}$. By averaging the white noise added in first step is assumed to cancle out each other.

In spite of repetitions, EEMD can be efficiently implemented by C/C++ library that supported multithreading [12]. As default configuration, the number of iteration N is chosen to be 250 and the number of sifting process is limited to 10.

2.3 Detrended Fluctuation Analysis (DFA)

From the previous process, EEMD decompose a single VAG signal into a set of IMFs. Among the set of IMFs, uncorrelated IMF should be discarded. The DFA technique provides a way to determine how correlated signal is, in term of a parameter α.

DFA is a method for detecting autocorrelation in time series with non-stationarities [13, 14]. It determines how correlated a signal is and measures this property in terms of a scalar parameter, α. The idea of this technique can be explained briefly as follows. Firstly, consider the correlation function

$$C(s) = \mathbf{E}[x(t)x(t+s)] \approx \frac{1}{N-s}\sum_{t=1}^{N-s} x(t)x(t+s)$$

where $x(t)$ is zero-mean signal. The method suggests that if x has a *long-range* correlation then $C(s)$ should obey a power law:

$$C(s) \propto s^{-\gamma} \tag{2}$$

where $0 < \gamma < 1$ and our goal is to determine γ, the correlation exponent, *indirectly* via the computation of a *fluctuation function*. This function, denoted by $F(s)$, is obtained by dividing the signal into parts of size s, removing a polynomial trend, and then computing its variance. The paper [13] states that:

- If the signal is long-range power-law as in (2), then the fluctuation function increases by a power law
$$F(s) \sim s^{1-\gamma/2} \quad \triangleq \quad s^{\alpha}.$$
where $\alpha = 1 - \gamma/2$ for $0 < \gamma < 1$,
- If the signal is uncorrelated or short-range correlated then $F(s) \sim s^{1/2}$ (see the detail of this claim in [13]), *i.e.*, $\alpha = 1/2$ indicates short-range correlation of the signal. For example, if the signal is white noise, its fluctuation exponent should be $\alpha = 1/2$.

In practice, we will calculate $F(s)$ from the DFA algorithm, determine the fluctuation exponent α and make a conclusion about the correlation property of this value. We now describe the DFA algorithm. Consider a time series $x(t)$ for $t = 1, 2, \ldots, N$ and its mean defined by $\bar{x} = (1/N)\sum_{t=1}^{N} x(t)$.

1. We integrate the time series $x(t)$.
$$y(t) = \sum_{k=1}^{t}[x(k) - \bar{x}],$$
and y is called the integrated time series.
2. The integrated time series is divided into boxes of equal length, s. In each box of length s, we perform a least-squares polynomial fit, called a *local trend*, to y. Let $y(i)$ denote

the ith chunk of y where $i = 1, 2, \ldots, \text{floor}(N/s)$. Therefore, the detrended time series is given by

$$Y(i) = y(i) - p(i), \quad i = 1, 2, \ldots, \text{floor}(N/s),$$

where $p(i)$ is the fitted polynomial (local trend) to the data in the ith chunk. The local trend can be choosen to be a fixed order of polynomial.

3. We compute the root-mean-square fluctuation of this integrated and detrended tiem series, called the *fluctuation function*:

$$F(s) = \sqrt{\frac{1}{N}\sum_{k=1}^{N}(Y(t))^2}.$$

4. Repeat the steps 2)-3) over all time scale s. It is shown that $F(s)$ will increase as the length of time scale, s, increases. We can plot $\log F(s)$ versus $\log s$ to see if the fluctuation function obeys a power law: $F(s) \propto s^{\alpha}$.

The interpretation of the correlation exponent, α, can be summarized according to [14] below.

- $0 < \alpha < 0.5$: the signal is correlated but large and small values are likely to alternate.
- $\alpha = 0.5$: white noise.
- $0.5 < \alpha < 1$: the signal has a long-range correlation.
- $\alpha = 1$: $1/f$ noise (or pink noise).
- $\alpha > 1$: the signal has a correlation explained by the power law.
- $\alpha = 1.5$: brown noise (integration of white noise).

As an example, for white noise such interpretation can be easily verified by inspecting equation 2. Since white noise has a normalized auto-correlation function of value one at lag zero and zero elsewhere, it yield $\gamma = 0$, *i.e.*, $\alpha = 0.5$. For an implementation, the algorithm for calculating DFA pairs $\big(\log(s), \log(F(s))\big)$ at lag s is provided by the Peng *et al.* [15]. Then α is easily calculated with slope when fitting line with the DFA pairs.

2.4 Short Time Fourier Transform

In loose definition, non-stationary can be seen as an inconsistency of frequency characteristics among flexion-extension cycle. Since VAG signal is non-stationary, a normal spectral analysis cannot capture the frequency characteristics that occurs only at specific cycle. In order to analyse VAG signals in broad context, the information of VAG signals should be obtained in both time and frequency.

Short Time Fourier Transform (STFT) analyses VAG signals in a part called a window [16]. In each window, signal can be assumed to be stationary. Such window is chosen to be

a function, so that a part of VAG signals taken into the window can be weighed. In each iteration, the window is moved by $\delta m = 25\%$ of the window length to analyse the next part of a VAG signals. The STFT of a time domain signal $y[n]$ is given by

$$Y(m,\omega) = \sum_{n=m}^{L-m-1} y[n]w[n-m]e^{-j\omega n}, \tag{3}$$

where $w[n]$ is a window function, $y[n]$ is VAG signals in time domain. The window is moved by varying $m \in M$, where $M = \{\delta m L k \,|\, 0 < k < \frac{1}{\delta m L}\}$. We choose Kaiser window of length L and window parameter β, given by

$$w(n) = \begin{cases} \frac{I_0\left(\sqrt{\beta(1-\frac{n-\alpha}{\alpha})^2}\right)}{I_0(\beta)} & ,0 \le n \le L-1, \\ 0 & ,\text{otherwise}, \end{cases}$$

where $\alpha = (L-1)/2$ and $I_0(\cdot)$ is zero-order modified Bessel function of the first kind. The parameter β is used to trade between main-lobe width and relative side-lobe amplitude. The Kaiser window reduces to the rectangular window when $\beta = 0$. To visualize frequency-domain information, consider power spectral density (PSD) in each window

Note that the PSD of $Y(m,\omega)$ is not divided by a number of all available data N because `fft` is implemented only within a window of length L. The power at k^{th} window is given by:

$$P(k)_{\text{dB}} = 10\log_{10}\left(\frac{|Y(k)|^2}{L}\right) = 20\log_{10}\left(\frac{|Y(k)|}{L}\right).$$

2.5 Spike extraction

Spike extraction is a process to preserve spikes by removing them before enter EEMD block and include them back after DFA block. From testing result in section 3.1, EEMD/DFA will strip off all spikes. Additionally removal of spike make observing the magnitude of signal easier. Since spike has about 2 times or more higher magnitude than those of VAG signals, it is difficult to view the fluctuation of VAG signals when plotting signal and spikes together in the same figure. Spike removal process plays an important role when observing correlation property of IMFs, as shown in testing result of section 3.1.1 and section 3.1.2.

From the high pass filtering process, the original signal y is filtered to be y_h and the low frequency motion trend which is filtered out is $y_l = y - y_h$. The spikes are considered to be the components that has a magnitude over maximum value of the motion trend. The value at spike $y(t_{\text{spike}})$ is extracted and written to another file and the value at that point is replaced with $y_l(t_{\text{spike}})$.

Despite the criterion, there still exists spikes in the signal. So that the second criterion is introduced. The filtered signal y_h whose value is over 2 times of the mean of 90 percentile are discarded, *i.e.*, set to zero. Figure 7a shows the example of the signal whose spikes are removed. It is clear that y_h are oscillate within a band. However there also signals that seems to be truncated as shown in Figure 7b.

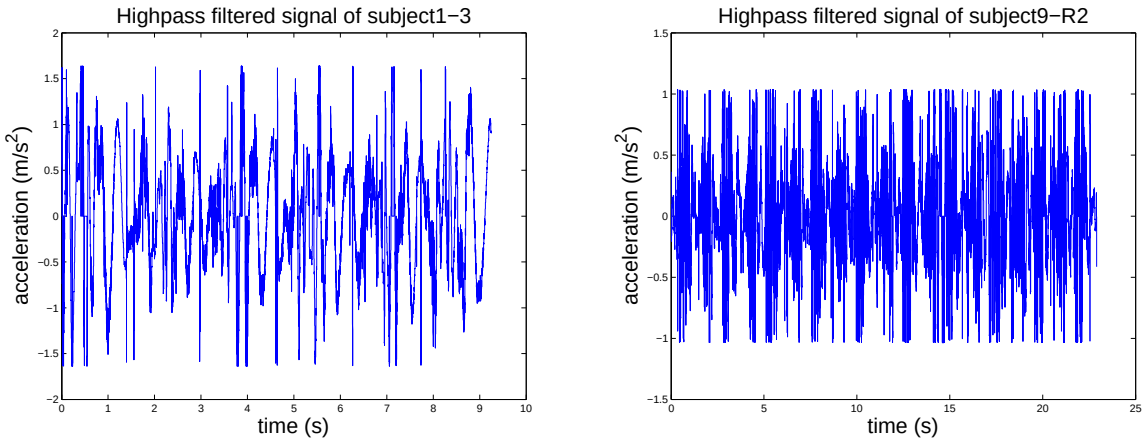

(a) (b)

Figure 7: Examples of signal whose spikes are removed with maximum motion trend and mean of 90 percentile criterion.

3 Experimental results

The section is divided into two subsections: (i) the first subsection is dedicated to illustrate the implementation and result of processing pipeline. A synthetic signal is used as an example input since it shows clearer results obtaining from the pipeline. (ii) the second subsection shows the result of signals after processing and theirs time-frequency analysis. Comparisons are draw from four important classes: (a) resurface, (b) non-resurface, (c) subject under different mesurement conditions and (d) subjects with knee rubbing sounds.

3.1 Noise removal of synthetic signal

This subsection will show the result of testing the EEMD/DFA methods with cosine function input $\cos(\omega)$ and $\cos(10\omega)$. It is expected that each components will be decomposed clearly by EEMD and discarded according to the α criterion, *i.e.*, discard $\alpha \leq 0.5$. The result should be close to the input without noise, *i.e.*, $\cos(\omega) + \cos(10\omega)$. This test aims to test if EEMD (Ensemble Emperical Mode Decomposition) can extract the white noise mixed in. After that, it is tested if DFA can label the IMFs having $\alpha = 0.5$ as suggested by the literature. The test case is divided into two parts according to synthetic signal used. They are (i) synthetic signal with spike and (ii) synthetic signal without spike.

3.1.1 Synthetic signal with spike

The synthetic signal y are generated consisting of four components $y = y_1 + y_2 + y_3 + y_4$. Properties associated to data acquisition are set to be similar to those of the real VAG signal, *i.e.*, sampling frequency $f_s = 12800Hz$, number of points collected $N = 200000$.

1. Motion trend: For simplicity we choose the motion trend to be cosine $y_1 = A\cos(\omega t)$ with amplitude $A = 1m/s^2$ and period $T = \frac{2\pi}{\omega} = 1s$.

2. Mid-frequency components: This components is added to check if EEMD can extract it into IMFs. We choose this component to be $y_2 = 0.1A\cos(10\omega t)$.

3. White noise: $y_3 \sim \mathcal{N}(\mu, \sigma^2)$ with $SNR = 80\%$ and $\mu = 0, \sigma^2 = 0.1$ is added to the motion trend.

4. Spike: Spike function y_4 are generated in a way that its location are Guassian with $\pm 3\sigma$ lying within $\pm T/8$ of each period of cosine trend and its amplitude obeys $A \sim \mathcal{N}(1, 0.5^2)$.

Then the synthetic signal is fed into the processing pipeline. The result of IMF and processed signal are shown in Figure 8 and 9. When comparing Figure 8a and 8b, it is clear that spikes are all removed and the signal become noticibly cleaner. Since spikes are not only concerned to be one of VAG signal characteristic but also concerned to have large portion in energy of VAG signal, spike should not be removed by EEMD process. Thus, there is the block to extract spikes and include them back in the processing pipeline.

According to section 2.3, there is an alternative to reconstruct the processed signal. If white noise is concerned to be the only noise in VAG signals, criterion is set to discard only IMFs having $\alpha = 0.5 \pm 0.1$. However, the result after processing in Figure 8c compared to the original signal in Figure 8a are not different.

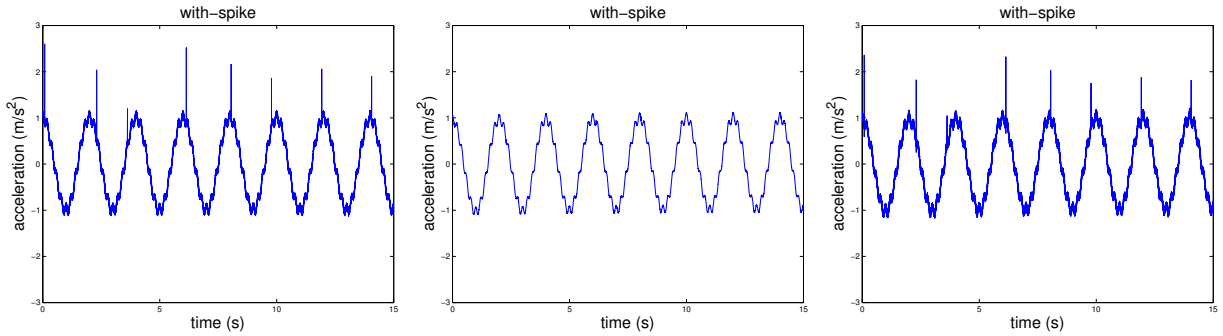

(a) Synthetic signal with spikes before processing

(b) Processed signal when discard IMFs having $\alpha \leq 0.5$

(c) Processed signal when discard IMFs having $\alpha = 0.5 \pm 0.1$

Figure 8: When choose criterion that discard $\alpha \leq 0.5$, all spike and significant amount of white noise are discarded yielding approximately $y_1 + y_2$.If the criterion that discard IMFs having $0.4 < \alpha < 0.6$ are chosen, C4 and C5 are the only modes that are discarded, as a result there is no significant difference for original synthesized signal and reconstructed signal, unnoticeable by raw eyes.

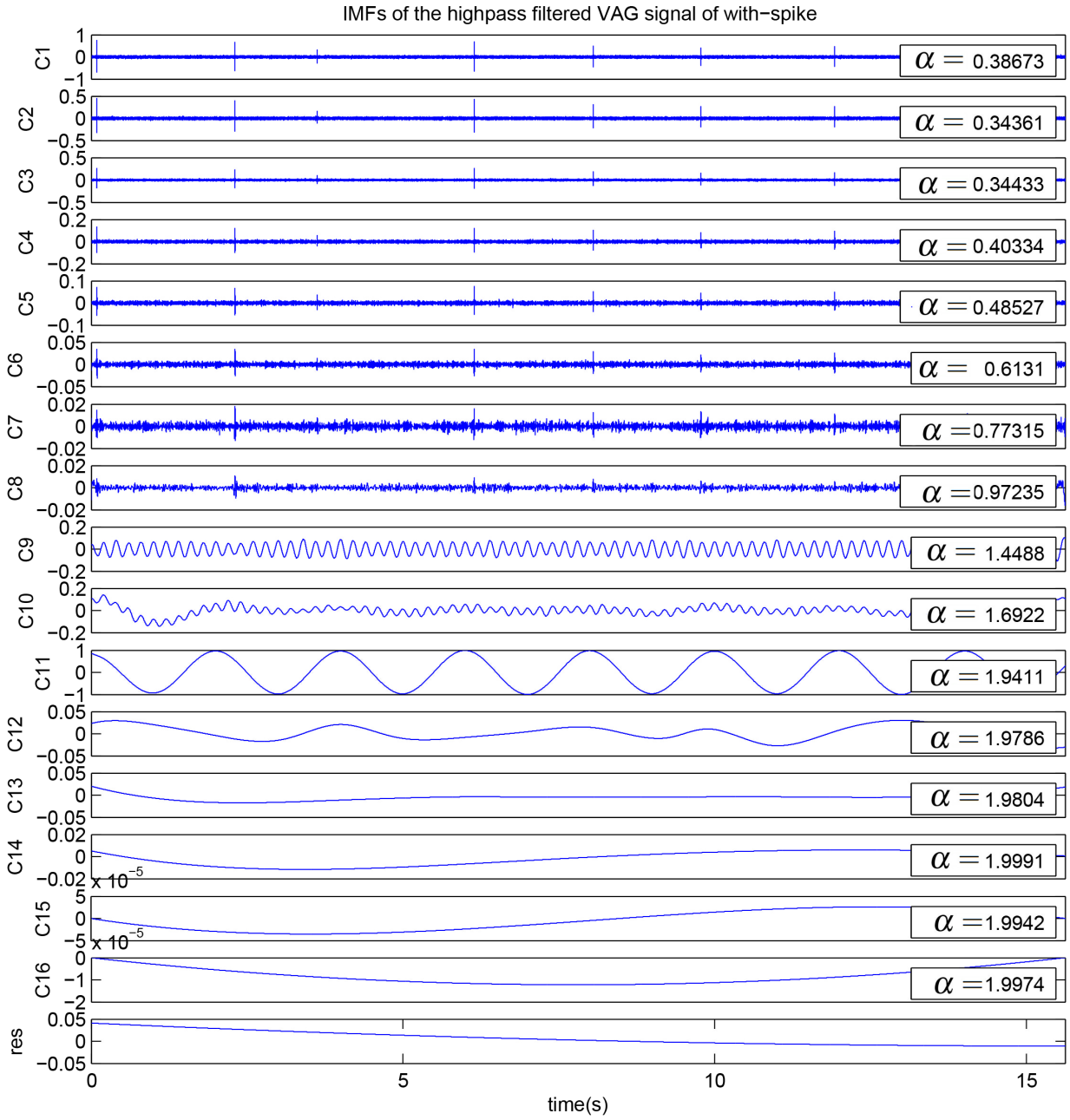

Figure 9: IMFs and corresponding α obtained from DFA of the synthetic signal with spike: As a result, EEMD correctly decomposes the y_1 and y_2. The IMF C9 and C10 are y_2 and C11 is y_1. However white noise y_3 are mixed with spikes y_4, which can be seen from C1 to C8. If assume that only y_1 and y_2 should be composed back, C1 to C8 should be all discarded. However not all IMF from C1 to C8 are white as indicated by α obtained from DFA. With the criterion that discard IMFs having $\alpha \leq 0.5$, C1 to C5 are discarded and the processed signal still has some IMF that seems to be random. Discarded IMFs C1 to C5 together have an amplitude about $2m/s^2$ which is in the same scale of the synthetic signal before entering the processing pipeline. On the contary, with the criterion that discard IMFs having $0.4 < \alpha < 0.6$, C4 and C5 are the only modes that are discarded, which together have amplitude in range of $0.3m/s^2$.

3.1.2 Synthetic signal without spike

From subsection 3.1.1, there are IMFs that has spikes mixed with white noise. Thus, spikes are removed to test if EEMD can decompose cleaner IMFs. The synthetic signal which fed in to the processing pipeline is $y = y_1 + y_2 + y_3$. As a result, Figure 11 shows that EEMD can decompose correctly which all modes that appears to be random are in C1 to C8. This is the reason to include spike extraction block into the processing pipeline. The criterion to discard IMFs are as same as in section 3.1.1: (i) discard IMFs having $\alpha \leq 0.5$ and (ii) discard IMFs having $\alpha = 0.5 \pm 0.1$. Similarly, with criterion (i) processed signal are cleaner noticable by raw eye. However with criterion (ii) signal appears to be as same as before it undergoes the process.

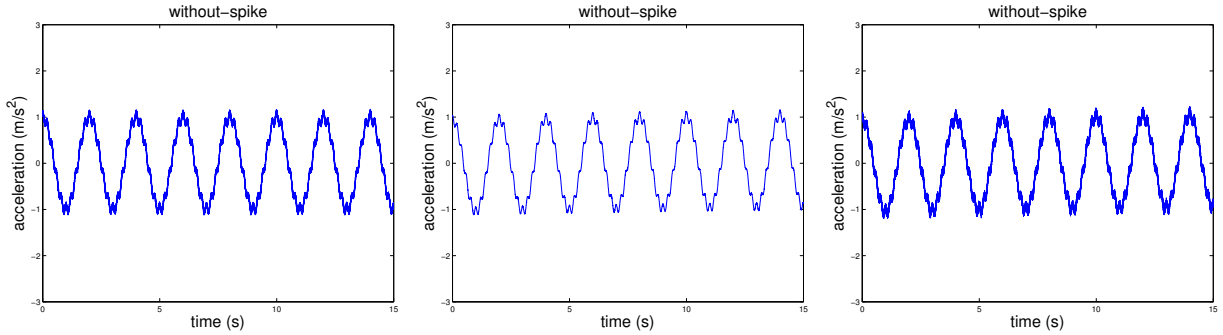

(a) Synthetic signal without spike before processing

(b) Processed signal when discard IMFs having $\alpha \leq 0.5$

(c) Processed signal when discard IMFs having $\alpha = 0.5 \pm 0.1$

Figure 10: Synthetic signal without spike. With criterion (i), C1 to C5 which made up about 75% of white noise generated are discarded, causing the processed signal noticably cleaner. However, with criterion (ii), only C5 is discarded so that the processed signal appears to be the same.

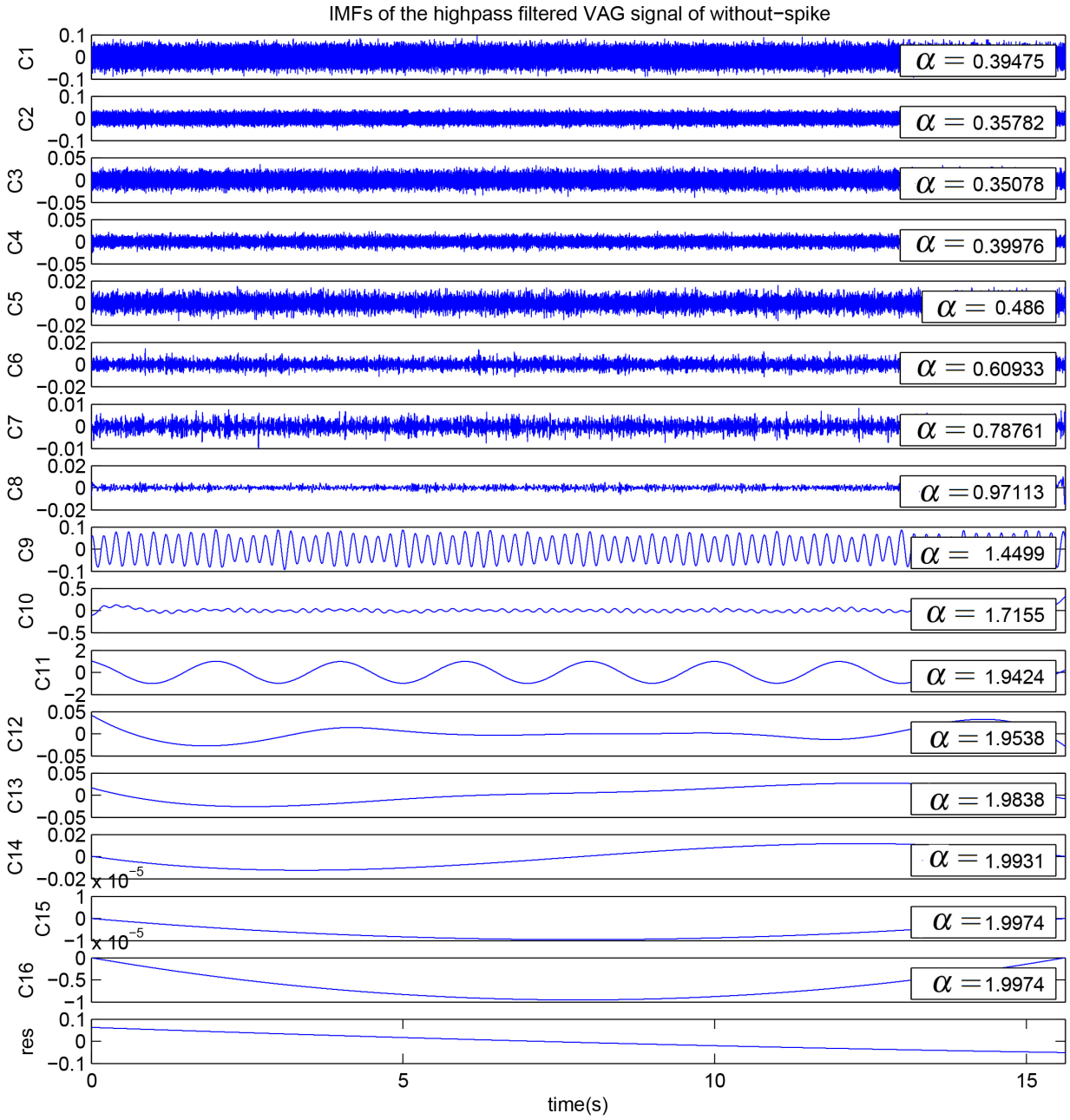

Figure 11: IMFs and corresponding α obtained from DFA of the synthetic signal with spike: The decomposition results are clearer than those of Figure 9 since there is no white noise y_3 mixing with spikes y_4. In this regard, EEMD correctly decomposes all modes in the synthetic signals. The results from synthetic signals with and without spikes share some similarities, *i.e.*, the IMF C9 and C10 are y_2 and C11 is y_1 and C1 to C8 appear to be random. If we sum IMFs from C1 to C8 and determine its α with DFA, it yields the signal that has $\alpha = 0.3925 < 0.5$. Likewise, with the criterion that discard IMFs having $\alpha \leq 0.5$, C1 to C5 are discarded and the processed signal still has some IMF that seems to be random. Discarded IMFs C1 to C5 together have an amplitude about $0.15m/s^2$, which is approximately equal to the white noise mixed in y_3. On the other hand, with the criterion that discard IMFs having $0.4 < \alpha < 0.6$, only C5 is discarded, which has amplitude only $0.01m/s^2$, *i.e.*, having a neglecgible result.

3.2 Results on processed VAG signals

This section will first introduce the resurface and non-resurface data set then show the result obtained from processing according to methodology in section 2.

Besides the VAG signals measured from each subject, there are further information on gender (male, female), age, side (left, right), condition (resurface, non-resurface) and time after surgery relative to date that VAG signals were measured. Description are all shown in Table 1. The flag N/A denotes that such information is not given.

Table 1: Additional subject description of the non-resurface and resurface classes. In the side column, L and R indicate left and right knee; and in the condition column R and N indicate resurface and non-resurface class respectively.

Subject	Gender	Age	Side	Condition	Time after surgery
1	F	N/A	L	R	6 Y
2	F	N/A	R	N/A	N/A
3	M	N/A	R	N	3 M
4	F	70	R	N	N/A
5	F	73	R	N	N/A
6	F	66	L	N	N/A
			R	N	1 Y
7	F	68	L	N	2 Y
			R	R	3 Y
8	M	N/A	R	N	6 M
9	F	69	L	R	10 Y
			R	R	10 Y
10	F	N/A	L	R	7 Y
			R	R	7 Y

Although there are factors that significantly vary among subject such as time after surgery, emphasis is on VAG signals and their time-frequency characteristics. The data set is fed to the processing pipeline with criterion to discard IMFs having

$$\alpha \leq 0.5. \tag{4}$$

The results obtained in time domain are in Figure 13 and theirs corresponding STFT is shown in Figure 14, which are analysed as follow:

1. Resurface and non-resurface class: From time results in Figure 13a and 13b and STFT results in Figure 14a and 14b, there is no distinct feature to separate the non-resurface and resurface groups from each other. It is expected that STFT results should be different to the extent that is shown in Figure 15, suggested in the literature [17]. If considering frequency features from the literature, frequency band power P1 (50-250 Hz) and P2 (250-450 Hz), normalized by signal length, are calculated from all 30 data sets as shown in Table 2. Despite that P1 and P2 of are different in mean value, standard deviation are too high to choose P1,P2 as classification features. Such ambiguity in classification is illustrated by Figure 12.

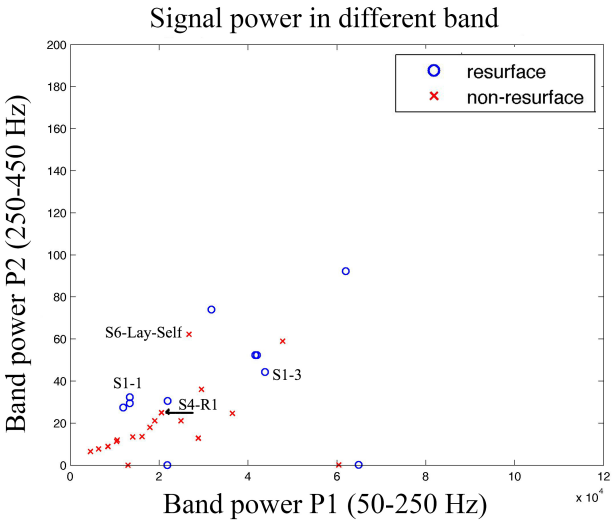

Figure 12: From all data set, resurface and non-resurface class are plotted according to their P1 and P2 properties. Obviously, there is no differences or even a cluster of data.

Table 2: Frequency band power comparison between resurface and non-resurface class

	P1 (50-250 Hz) (W)	P2 (250-450 Hz) (W)
Resurface	$(3.9252 \pm 2.6928) \times 10^4$	52.2507 ± 51.2711
Non-resurface	$(2.1963 \pm 1.4726) \times 10^4$	19.6485 ± 17.3809

2. Variation on the measuring condition: Consider an interesting result of subject 6 whose VAG signals were measured in various condition labeled by `S6 R1, S6 R3 Freefall, S6 R4 Lay Assist` with description:

   - Freefall: Subject was sitting on a chair, moving the knee up and let it fall down freely to the original position.
   - Lay Assist: Subject was lying on a bed and moved the knee up with assistance.
   - Lay Self: Subject was lying on a bed and moved the knee up by him/herself.

   During the measurement process, the physician heard *crepitus* sound which is an indication of degraded knee as the subject was lying on a bed (`Lay Self`). Although VAG signals of `S6 R1, S6 R3 Freefall`, `S6 R4 Lay Assist` and `S6 R5 Lay Self` are from subject 6's right knee, physician only heard crepitus sound under Lay Self condition.

3. Results from patients with knee sound: Since there are no differences between resurface and non-resurface class, we hypothesize that the feature characteristics of the signal should depend upon individual and one's knee condition. Thus, the results from subject 1,4,6 which physician heard the cracking sound are chosen for a comparison. Despite no significant difference in Figure 14d, power of signals of this type is higher than the other class especially from subject 6, $3.64 \times 10^4 W$, which is the highest and about one standard deviation higher than the average of $2.89 \times 10^4 W$.

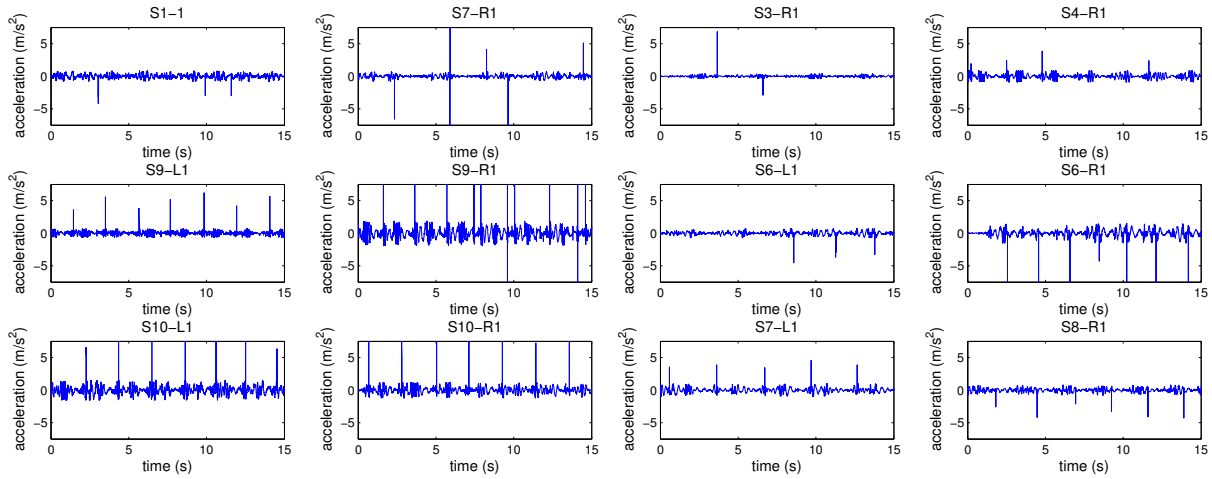

(a) Resurface (b) Non-resurface

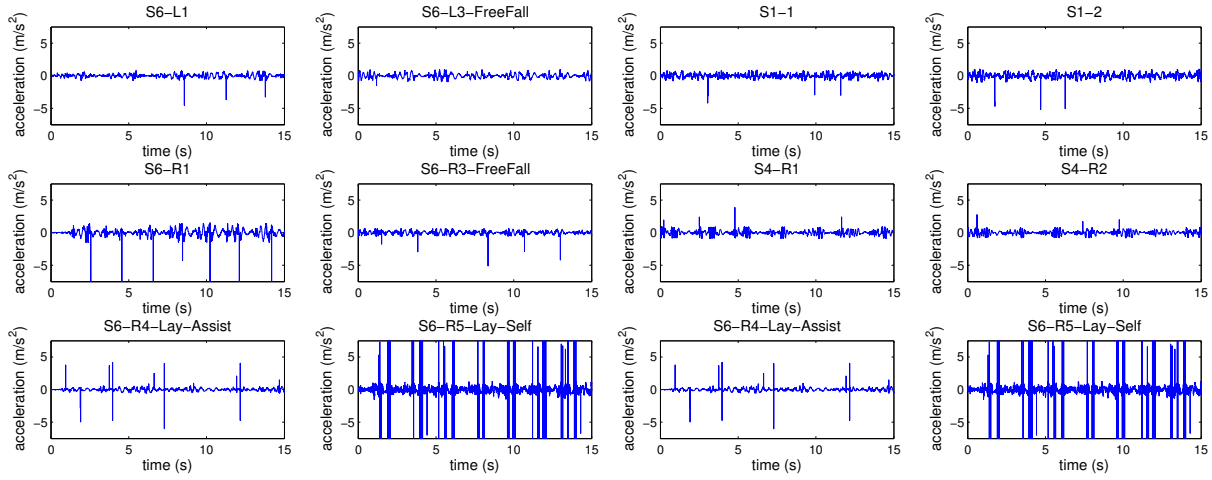

(c) Subject 6 under different conditions (d) Subjects with sound

Figure 13: Time-domain result of processed signals. By raw eye, both resurface and non-resurface classes are not different. Even in the same class, there seems to have no common characteristics. Contradict to our expectation, not all signals of subjects with cracking sound also have high magnitude. Only subject-6-Lay-self does. Measurement under different condition give a significant different signal. This results are the same without processing.

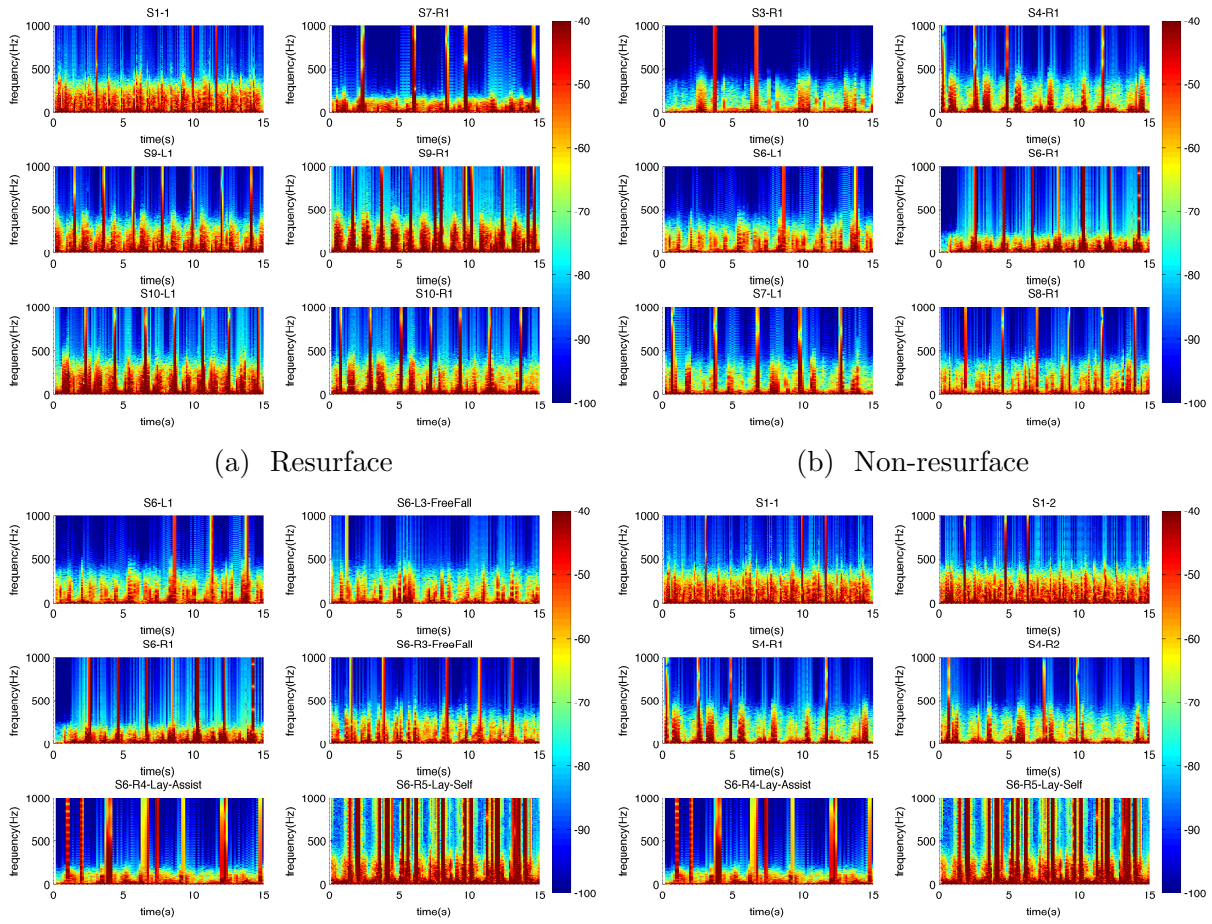

(a) Resurface

(b) Non-resurface

(c) Subject 6 under different conditions

(d) Subjects with sound

Figure 14: STFT result of processed signal: Energy of all class concentrates on the band $0-500$Hz. Spikes included back are clear as shown in red ridge spreading across all frequencies.

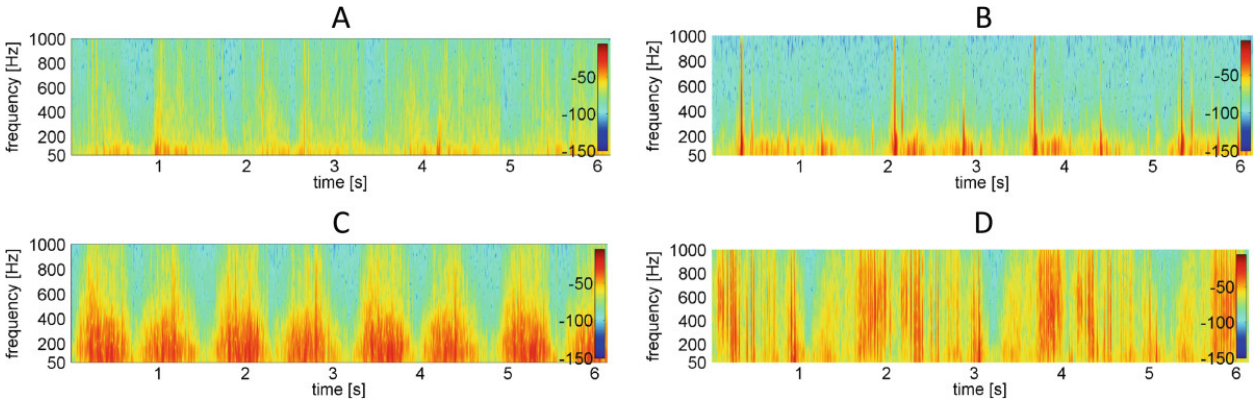

Figure 15: STFT results from the literature [17], which are obtained from (A), control healthy knee; (B) knee with lateral patella compression syndrome; (C) knee with chondromalacia; (D) knee with patellofemoral joint osteoarthritis. There is distinct difference not only between control group and degraded knee (A and B,C,D) but also among knee diseases (B,C and D).

4 Conclusion

In this project VAG signal of class resurface and non-resurface are studied. Since raw VAG signals contain motion trend and noise, the signals should be processed before analysing. The processing pipeline contains four steps: (i) remove motion trend with high-pass filter. (ii) extract spikes and include back after EEMD/DFA block to avoid EEMD/DFA to eliminate spikes. (iii) decompose with EEMD, non-stationary signal processing technique to obtain a set of IMFs (iv) analyse each IMFs correlation properties in term of α then discard IMFs having $\alpha \leq 0.5$. Finally, the processed signal is analysed with STFT to observe its time-frequency characteristics. Differences of STFT results under different measurement condition are observed. Contary to the hypothesis, only one subjects with cracking sounds has a distinct STFT result. Nevertheless, there is no clear distinction results between non-resurface and resurface class both in time and time-frequency domain, it can be concluded that for this data set there is no differences between non-resurface and resurface class.

5 Acknowledgment

This project is a part of research group initiated and led by Jitkomut Songsiri PhD, Department of Electrical Engineering, Chulalongkorn University, Kakkanan Srungbunmee PhD, Center of Data Mining and Biomedical Informatics, Mahidol University and Satit Thiengwittayaporn MD, Department of Orthopaedics Surgery, Bangkok Metropolitan Administration Medical College and Vajira Hospital. We wish to thank to the group not only for the data but also for valuable advice given along one year time of the project.

References

[1] K. Barbour, C. Helmick, K. Theis, L. Murphy, J. Hootman, and T. Brady, "Prevalence of doctor-diagnosed arthritis and arthritis-attributable activity limitation in united states, 2010–2012," *Morbidity and Mortality Weekly Report*, 2013.

[2] G. McCoy, J. McCrea, D. Beverland, W. Kernohan, and R. Mollan, "Vibration arthrography as a diagnostic aid in diseases of the knee. a preliminary report," *The bone and joint journal*, vol. 69-B, pp. 288–293, March 1987.

[3] Blodgett and W. Ernest, "Auscultation of the knee joint," *The Boston Medical and Surgical Journal*, vol. 146, no. 3, pp. 63–66, 1902.

[4] Y.-T. Zhang, C. B. Frank, R. Rangayyan, and G. Bell, "Mathematical modeling and spectrum analysis of the physiological patello-femoral pulse train produced by slow knee movement," *Biomedical Engineering, IEEE Transactions on*, vol. 39, pp. 971–979, Sept 1992.

[5] S. Tavathia, R. Rangayyan, C. B. Frank, G. Bell, K. Ladly, and Y.-T. Zhang, "Analysis of knee vibration signals using linear prediction," *Biomedical Engineering, IEEE Transactions on*, vol. 39, pp. 959–970, Sept 1992.

[6] W. G. Kernohan, D. E. Beverland, G. F. Mccoy, S. N. Shaw, R. G. Wallace, G. C. Mccullagh, and R. A. Mollan, "The diagnostic potential of vibration arthrography.," *Clinical orthopaedics and related research*, vol. 210, pp. 106–112, 1986.

[7] M. Chu, I. Gradisar, M. Railey, and G. Bowling, "An Electro-acoustical technique for the detection of knee joint noise," *Medical research engineering*, vol. 12(1), pp. 18–20, 1976.

[8] N. Huang, S. Zheng, S. Long, M. Wu, H. Shih, Q. Zheng, N. Yen, C. Tung, and H. Liu, "The Empirical mode decomposition and the Hilbert spectrum for nonlinear and non-stationary time series analysis," *Proceedings of the Royal Society of London A: Mathematical, Physical and Engineering Sciences*, vol. 454, no. 1971, pp. 903–995, 1998.

[9] K. M. Chang, "Arrhythmia ECG noise reduction by ensemble empirical mode decomposition," *Sensors (Basel)*, vol. 10, no. 6, pp. 6063–6080, 2010.

[10] C.-K. Peng, S. V. Buldyrev, S. Havlin, M. Simons, H. E. Stanley, and A. L. Goldberger, "Mosaic organization of dna nucleotides," *Phys. Rev. E*, vol. 49, pp. 1685–1689, Feb 1994.

[11] N. Huang and Z. Wu, "A Review on Hilbert-Huang transform: Method and its applications to geophysical studies," *Reviews of Geophysics*, vol. 46, no. 2, 2008.

[12] P. J. J. Luukko, J. Helske, and E. Räsänen, "Introducing libeemd: a program package for performing the ensemble empirical mode decomposition," *Computational Statistics*, vol. 31, no. 2, pp. 545–557, 2015.

[13] J. Kantelhardt, E. Koscielny-Bunde, H. Rego, S. Havlin, and A. Bunde, "Detecting long-range correlations with detrended fluctuation analysis," *Physica A: Statistical Mechanics and its Applications*, vol. 295, no. 3, pp. 441–454, 2001.

[14] C.-K. Peng, S. Havlin, H. E. Stanley, and A. L. Goldberger, "Quantification of scaling exponents and crossover phenomena in nonstationary heartbeat time series," *Chaos: An Interdisciplinary Journal of Nonlinear Science*, vol. 5, no. 1, pp. 82–87, 1995.

[15] A. L. Goldberger, L. A. N. Amaral, L. Glass, J. M. Hausdorff, P. C. Ivanov, R. G. Mark, J. E. Mietus, G. B. Moody, C.-K. Peng, and H. E. Stanley, "PhysioBank, PhysioToolkit, and PhysioNet: Components of a new research resource for complex physiologic signals," *Circulation*, vol. 101, no. 23, pp. e215–e220, 2000 (June 13). Circulation Electronic Pages: http://circ.ahajournals.org/cgi/content/full/101/23/e215 PMID:1085218; doi: 10.1161/01.CIR.101.23.e215.

[16] A. V. Oppenheim, R. W. Schaffer, and J. R. Buck, *Discrete Time Signal Processing*. Upper Saddle River, New Jersey: Prentice-Hall, 2 ed., 1999.

[17] D. Baczkowicz and E. Majorczyk, "Joint motion quality in vibroacoustic signal analysis for patients with patellofemoral joint disorders," *BMC Musculoskeletal Disorders*, vol. 15, no. 1, pp. 1–7, 2014.